

Fundamental limit of 1/f frequency noise in semiconductor lasers due to mechanical thermal noise

K. Numata,^{1,2,*} and J. Camp²

¹*Department of Astronomy, University of Maryland, College Park, Maryland, 20742, USA*

²*NASA Goddard Space Flight Center, Greenbelt, Maryland, 20771, USA*

**email: kenji.numata@nasa.gov*

So-called 1/f noise has power spectral density inversely proportional to frequency, and is observed in many physical processes. Single longitudinal-mode semiconductor lasers, used in variety of interferometric sensing applications, as well as coherent communications, exhibit 1/f frequency noise at low frequency (typically below 100kHz)^{1, 2, 3, 4, 5, 6, 7, 8, 9, 10}. Here we evaluate mechanical thermal noise due to mechanical dissipation in semiconductor laser components and give a plausible explanation for the widely-observed 1/f frequency noise, applying a methodology developed for fixed-spacer cavities for laser frequency stabilization. Semiconductor-laser's short cavity, small beam radius, and lossy components are expected to emphasize thermal-noise-limited frequency noise. Our simple model largely explains the different 1/f noise levels observed in various semiconductor lasers, and provides a framework where the noise may be reduced with proper design.

Power spectral density of the frequency noise of the semiconductor laser has two components¹: frequency independent component (white noise) at high frequency, which is understood as fluctuation due to spontaneous emission, and the 1/f component at lower frequency. The 1/f component was found to be independent of laser injection current^{1, 8}, and to become enhanced when materials are degraded at high temperatures^{2, 3}. Several processes have been conjectured to be related to the origin of the 1/f noise, for example, the free electron generation-recombination associated with material defects^{2, 3}. Supporting this theory, a correlation between the magnitude of the 1/f noise and the leakage current was indicated in some semiconductor lasers⁵. However, no theory yet presented can associate the 1/f noise level with known design parameters.

In contrast, mechanical thermal fluctuation (Brownian motion) is realized to be one of the fundamental noise sources in precision optical measurements. Thermal noise is caused by the energy stochastically flowing to and from the heat bath. Electrical noise in resistors (electrical loss) is a famous example. The 1/f mechanical thermal noise in suspended mirrors was experimentally observed at wide frequency range (100Hz~100kHz)^{11, 12}. It was also found to be a limiting noise source in the use of optical cavities for frequency stabilization of lasers^{13, 14, 15, 16, 17}. Compared to macroscopic optical cavities, the semiconductor laser cavity has shorter length and smaller beam radius, which exaggerate the effect of the mechanical thermal noise on the output frequency. Due to the small size of the semiconductor laser system, two other temperature-related noise sources, thermal noise associated with thermoelastic damping^{18, 19} and the thermodynamical path-length fluctuation within optical media²⁰, have flat frequency spectrum at

the frequency of interest, and they are not responsible for the 1/f noise. The background intrinsic mechanical loss, ϕ , which is an inverse of mechanical quality factor and considered to be constant against frequency, has more relevance.

The fluctuation dissipation theorem (FDT)²¹ relates the power spectral density of observable quantity X, $G_X(f)$, and the dissipated energy, $W_{diss}(f)$, under the conjugate cyclic force, $F_0 \cos(2\pi f t) \mathbf{P}(\mathbf{r})$, as²²

$$G_X(f) = \frac{2k_B T W_{diss}(f)}{\pi^2 f^2 F_0^2}. \quad (1)$$

Here, k_B is the Boltzmann constant, T is the temperature, f is the frequency, and $\mathbf{P}(\mathbf{r})$ is the weighing function. According to the FDT, thermal-noise-limited frequency noise of an optical cavity comprised of a fixed-spacer supporting two mirrors (as shown in Figure 1, A)) is modeled as¹³

$$\sqrt{G_v(f)} \approx \frac{c}{L\lambda} \left\{ \frac{4k_B T}{\pi f} \left[\frac{L}{3AE_{sp}} \phi_{sp} + \frac{1-\sigma^2}{\sqrt{\pi} w_0 E_{sub}} \phi_{sub} \left(1 + \frac{2}{\sqrt{\pi}} \frac{1-2\sigma}{1-\sigma} \frac{\phi_{coat} d}{\phi_{sub} w_0} \right) \right] \right\}^{\frac{1}{2}}, \quad (2)$$

where $\sqrt{G_v}$ is the frequency noise, c is the speed of light, λ is the wavelength, L is the cavity (spacer) length, E_{sp}/E_{sub} are the Young's modulus of the spacer/mirror substrate, A is the cross sectional area of the spacer, σ is the Poisson's ratio of the mirror substrate, w_0 is the $1/e^2$ Gaussian beam radius, d is the thickness of the coating, and $\phi_{sp}/\phi_{sub}/\phi_{coat}$ are the mechanical loss of the spacer/substrate/coatings. The term with parenthesis $\{ \}$ represents the displacement noise, and $c/(L\lambda)$ represents length-to-frequency conversion factor obtained from the resonance condition, $2L=N\lambda$, where N is an integer. The first term inside the parenthesis $\{ \}$ represents spacer contribution, and the second term represents mirror contribution, corrected by the factor inside $()$ to treat coatings. This mirror *surface* fluctuation is analytically calculated, assuming Gaussian weighing and very thin coating on the substrate that occupies infinite-half space^{23, 24, 25}.

In semiconductor lasers, the geometry involved is a very small beam directed to a reflective substrate (or thicker coatings) through a transmissive substrate (as shown in Figure 1, B)). Thus we consider the thermal noise *inside* the substrate with the following expression, by neglecting the mechanical difference between the two substrates, and by treating the system as infinite space,

$$\sqrt{G_v(f)} \approx \frac{c}{L\lambda} \left\{ \frac{4k_B T}{\pi f} \left[\frac{L}{3AE_{sp}} \phi_{sp} + \frac{1}{8} \frac{(3-4\sigma)(1+\sigma)}{\sqrt{\pi} w_0 E_{sub}} \phi_{sub} \right] \right\}^{\frac{1}{2}}. \quad (3)$$

The factor difference in the mirror term, $(1-\sigma^2)$ and $(3-4\sigma)(1+\sigma)/8$, comes from the difference in the Green's tensors for the equations of equilibrium of infinite-half and infinite spaces²⁶. The small beam radius w_0 enhances the thermal noise, since it does not average any longer-scale fluctuations out within the beam illuminated area. We now apply this formulism to evaluate thermal noise in specific semiconductor lasers. As typical values, we adopt $\lambda=1550\text{nm}$ and $T=300\text{K}$. For semiconductor materials we use $\sigma=0.3$, $E=80\text{GPa}$ (GaAs), and $\phi=10^{-3}$, whose

validity will be discussed later. Other parameters are dependent on each laser design. In order to check the validity of equation (3), and to evaluate the effect of epoxy and conductive layers (including gold coating and bonding pad on the gain chip), we numerically calculated the thermal noise using the finite element method. In this analysis, forces were applied to laser models, and then equation (1) directly converted the dissipated energy into the thermal noise.

The vertical-cavity surface-emitting laser (VCSEL) achieves single-mode lasing by adopting a very short cavity length. Figure 2, A) shows a structure of VCSEL. VCSEL has cavity mirrors composed of semiconductor distributed Bragg reflector (DBR) and/or silica-alumina coating. Although the cavity is composed of multiple layers of different semiconductor materials, we regard the cavity “spacer” and the mirror “substrate” as being made of uniform material ($E_{sp}=E_{sub}=80\text{GPa}$, $\phi_{sp}=\phi_{sub}=10^{-3}$). As typical VCSEL design, we adopt $L=5\mu\text{m}$, $A=(10\mu\text{m})^2$, and $w_0=3\mu\text{m}$. Then equation (3) sets thermal noise limit of $8.4\text{kHz}/\sqrt{\text{Hz}}$ at $f=100\text{Hz}$. Our numerical calculation validated this result. In Figure 2, B) we compare the experimental results and the calculation showing contribution from each component. The experimental result is within factor ~ 10 of the calculation below 1kHz , where the measured spectrum is not limited by the white noise.

The distributed-feedback (DFB) laser has a distributed mirror with internal optical gain, which effectively selects a lasing wavelength that satisfies Bragg reflection condition. Figure 3, A) shows a structure of DFB laser. The light is confined within the semiconductor waveguide, typically supporting an elliptic beam ($\sim 1\mu\text{m}\times 1.5\mu\text{m}$). Laser operation is achieved with anti-reflective (AR) coated end faces of the chip (typically $\sim 400\mu\text{m}$ in length). We model the cavity as composed of reflective substrates connected by the same material (like the VCSEL model). As typical DFB laser design, we adopt effective cavity length $L=50\mu\text{m}$, $A=(100\mu\text{m})^2$, and $w_0=1\mu\text{m}$. Then equation (3) sets $1.3\text{kHz}/\sqrt{\text{Hz}}$ thermal noise limit at $f=100\text{Hz}$, with smaller contributions from the spacer term than the mirror term. In Figure 3, B), we compare the experimental results and the numerically calculated result. When the effect of the lossy conductive layer ($\phi=10^{-1}$) is considered, the calculated result was within factor ~ 3 of the measurement. The conductive layer has larger effect since it is close to the waveguided beam (typically $1\sim 2\mu\text{m}$ beneath the conductive layer in the gain media).

External-cavity diode laser (ECL) uses external frequency-selecting mirror and a semiconductor gain chip. The rear end of the gain chip uses a high-reflectivity (HR) coating. An external mirror is typically provided by a fiber Bragg grating in integrated ECLs. Figure 4, A) shows structure of such ECL. The components are fixed on stiff submounts with epoxy. The thermal noise contribution from the waveguided gain chip (with coatings) is about half of the DFB laser, since it has similar beam radius ($w_0\sim 1\mu\text{m}$) and only one reflection. In the external mirror, the beam has larger radius ($w_0\sim 5\mu\text{m}$). By neglecting the the external mirror, and by scaling the DFB laser noise with the typical effective cavity length of ECL, $L=5\text{mm}$, the thermal noise limit set by the gain chip becomes $9.1\text{Hz}/\sqrt{\text{Hz}}$ ($=1.3\text{kHz}/\sqrt{\text{Hz}} / \sqrt{2} / (5\text{mm}/5\mu\text{m})$). In Figure 4, B), we compare the experimental results and the numerically calculated result, including effects of conductive layer and epoxy. The experimental results are factor ~ 10 away from the calculated thermal noise limit, in which the conductive layer could have the largest contribution. The larger discrepancy seen for ECL may be due to an optimistic assumption of loss value of the epoxy ($\phi=10^{-2}$).

We believe $\phi=10^{-3}$ is a reasonable assumption for the semiconductor materials, since ϕ s of 1/500 for GaAs²⁷, 1/300 for InGaAsP²⁸, 1/890 for InP²⁹, and 1/5000 for AlGaAs³⁰ have been reported. However, the surface loss, the grating structure, and the stacked semiconductor structure may elevate the total mechanical loss considerably. Loss values of epoxy and conductive layer have larger uncertainty. In addition, semiconductor lasers have more complicated resonance condition than simple passive cavities due to wavelength-dependent gain, optical loss, and detuning (difference between lasing wavelength and Bragg reflection peak wavelength). Since the displacement-to-frequency conversion factor in equation (3) is affected by these temperature sensitive effects, the 1/f noise power may not be proportional to 1/T. This may present a limit on the experimental validity of the model we have presented.

Nevertheless, compared to the previous theories based on electrical noise, our thermal noise model shows better quantitative agreement to the observed 1/f frequency noise. Achieving better frequency noise performance for semiconductor lasers will require solving the difficult problem of reducing thermal noise in small mechanical systems. We think it can be done by 1) using longer cavity, 2) operating at low temperature, 3) adopting larger beam, 4) adopting low-loss materials, and 5) using less number of lossy components and putting them away from the beam. We believe our results may help wide communities realize the importance of the mechanical thermal noise.

References

1. Kikuchi, K., *Effect of 1/f-type FM noise on semiconductor-laser linewidth residual in high-power limit*, IEEE J. Quant. Electron. **25**, 684-688 (1989).
2. Fukuda, M., Hirono, T., Kurosaki, T., & Kano, F., *1/f noise behavior in semiconductor-laser degradation*, IEEE Photon. Tech. Lett. **5**, 1165-1167 (1993).
3. Fukuda, M., Hirono, T., Kurosaki, T., & Kano, F., *Correlation between 1/f noise and semiconductor laser degradation*, Quality and Reliability engineering International, **10**, 351-353 (1994).
4. Garmash, A., Morozov, V. N., Semenov, A. T., Sumarokov, M. A., & Shidlovski, V. R., *Leakage currents and 1/f noise in buried in GaAs/InP heterostructure lasers*, Sov. J. Quant. Electron. **20**, 882-886 (1990).
5. Bartolo, R. E., Kirkendall, C. K., Kupersmidt, V., & Siala, S., *Achieving narrow linewidth low-phase noise external cavity semiconductor lasers through the reduction of 1/f noise*, Proc. SPIE **6133**, 61330I (2006).
6. Cliche, J.-F., Allard, M., & Têtu, M., *High-power and ultranarrow DFB laser: the effect of linewidth reduction systems on coherence length and interferometer noise*, Proc. SPIE **6216**, 62160C (2006).
7. Bartolo, R. E., Tveten, A., & Kirkendall, C. K., *The quest for inexpensive, compact, low phase noise laser sources for fiber optic sensing applications*, Proc. SPIE **7503**, 750370-1 (2009).
8. Tourenç, J. P., Signoret, P., Myara, M., Alabedra, E., Marin, F., & Choquette, K. D., *Frequency noise in 850nm selectively oxidized VCSELs*, Fluct. Noise Lett. **3**, L407-L412 (2003).
9. Viciani, S., & Marin, R., *Frequency noise and lineshape of VCSELs*, Proc. SPIE **4286**, 109-118 (2001).

10. Numata, K., Camp, J., Krainak, M. A., & Stolpner, L., *Performance of planar-waveguide external cavity laser for precision measurements*, Opt. Exp. **18**, 22781-22788 (2010).
11. Numata, K., Ando, M., Yamamoto, K., Otsuka, S., & Tsubono, K., *Wide-band direct measurement of thermal fluctuations in an interferometer*, Phys. Rev. Lett. **91**, 260602 (2003).
12. Black, E. D., Villar, A., Barbary, K., Bushmaker, A., Heefner, J., Kawamura, S., Kawazoe, F., Matone, L., Meidt, S., Rao, S. R., Schulz, K., Zhang, M., & Libbrecht, K. G., *Direct observation of broadband coating thermal noise in a suspended interferometer*, Phys. Lett. A **328**, 1-5 (2004).
13. Numata, K., Kemery, A., & Camp, J., *Thermal-noise limit in the frequency stabilization of lasers with rigid cavities*, Phys. Rev. Lett. **93**, 250602 (2004).
14. Notcutt, M. Ma, L.-S., Ludlow, A. D., Foreman, S. M., Ye, J., & Hall, J. L., *Contribution of thermal noise to frequency stability of rigid optical cavity via Hertz-linewidth lasers*, Phys. Rev. A **73**, 031804(R) (2006).
15. Ludlow, D., Huang, X., Notcutt, M., Zanon-Willette, T., Foreman, S. M., Boyd, M. M., Blatt, S., & Ye, J., *Compact, thermal-noise-limited optical cavity for diode laser stabilization at 1×10^{-15}* , Opt. Lett. **32**, 641-643 (2007).
16. Webster, S. A., Oxborrow, M., Pugla, S., Millo, J., & Gill, P., *Thermal-noise-limited optical cavity*, Phys. Rev. A **77**, 033847 (2008).
17. Jiang, Y. Y., Ludlow, A. D., Lemke, N. D., Fox, R. W., Sherman, J. A., Ma, L.-S., & Oates, C. W., *Making optical atomic clocks more stable with 10^{-16} -level laser stabilization*, Nature Photonics, (2011), doi:10.1038/nphoton.2010.313.
18. Zener, C., *Internal Friction in Solids. I. Theory of Internal friction in reeds*, Phys. Rev. **52**, 230-235 (1937).
19. Braginsky, V.B., Gorodetsky, M.L., & Vyatchanin, S.P., *Thermodynamical fluctuations and photo-thermal shot noise in gravitational wave antennae*, Phys. Lett. A **264**, 1-10 (1999).
20. Glenn, W. H., *Noise in interferometric optical systems: an optical Nyquist theorem*, IEEE J. of Quant. Electron. **25**, 1218-1224 (1989).
21. Callen, H. B. & Greene, R. F., *On a Theorem of irreversible thermodynamics*, Phys. Rev. **86**, 702-710 (1952).
22. Levin, Y., *Internal thermal noise in the LIGO test masses: A direct approach*, Phys. Rev. D **57**, 659-663 (1998).
23. Bondu, F., Hello, P., & Vinet, J.-Y., *Thermal noise in mirrors of interferometric gravitational wave antennae*, Phys. Lett. A **246**, 227-236 (1998).
24. Nakagawa, N., Gretarsson, A. M., Gustafson, E. K., & Fejer, M. M., *Thermal noise in half-infinite mirrors with nonuniform loss: A slab of excess loss in a half-infinite mirror*, Phys. Rev. D **65**, 102001 (2002).
25. Gurkovsky, A. & Vyatchanin, S., *The thermal noise in multilayer coating*, Phys. Lett. A **374**, 3267-3274 (2010).
26. Landau, L.D. & Lifshitz, E.M., *Theory of Elasticity, third edition*, Butterworth-Heinemann, Oxford (1986).
27. Cole, G. D., Ph.D thesis, *MEMS-tunable vertical-cavity SOAs*, University of California, Santa Barbara, December (2005).
28. Siwak, N., Fan, X., Hines, D., Williams, E., Goldsman, N., & Ghodssi, R., *Chemical sensor utilizing indium phosphide cantilevers and pentacene as a functionalization layer*,

- Micro Electro Mechanical Systems, 2007. MEMS. IEEE 20th International Conference on, 489-492 (2007).
29. Gavartin, E., Braive, R., Sagnes, I., Arcizet, O., Beveratos, A., Kippenberg, T. J., & Robert-Philip, I., *Optomechanical coupling in a two-dimensional photonic crystal defect cavity*, arXiv:1011.6400v1.
 30. Cole, G. D., Gröblacher, S., Gugler, K., Gigan, S., & Aspelmeyer, M., *Monocrystalline $Al_xGa_{1-x}As$ heterostructures for high-reflectivity high- Q micromechanical resonators in the megahertz regime*, Appl. Phys. Lett. **92**, 261108 (2008).

Acknowledgements

Authors would like to thank Prof. Kimio Tsubono at the University of Tokyo (Tokyo, Japan), Dr. Lew Stolpner, Dr. Mazin Alalusi at Redfern Integrated Optics (California, USA), Dr. Kazuhiro Yamamoto at the Institute for Cosmic Ray Research (Kashiwa, Japan), and Dr. Robert Bartolo at the Naval Research Laboratory (Washington DC, USA) for their useful comments.

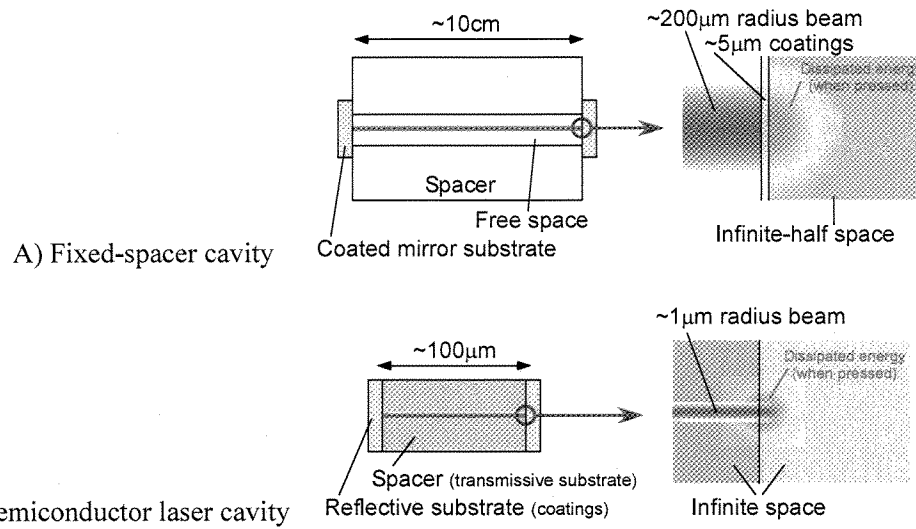
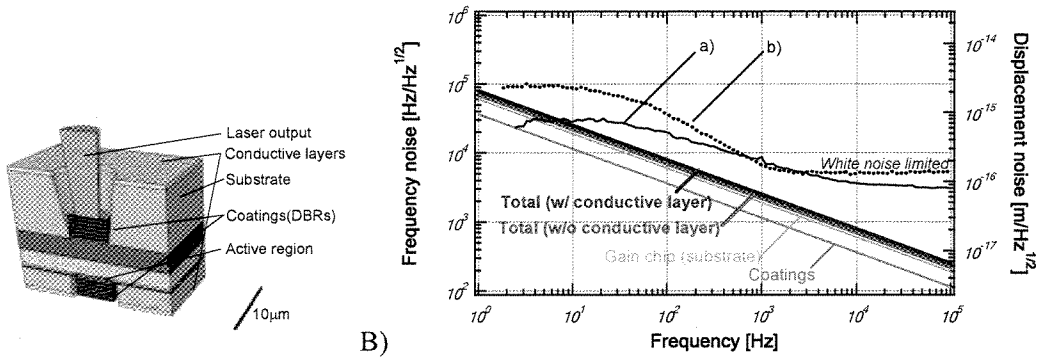


Figure 1 | Typical structure, size, and situation around the beam spot in A) fixed-spacer cavity for laser frequency stabilization and B) semiconductor laser cavity. In the fixed-spacer cavity, the mirror substrate can be treated as an infinite-half space when evaluating thermal noise by applying a force, which has same weighing as laser power distribution, by calculating the dissipated energy, and by applying the FDT. In contrast, the semiconductor cavity should be treated as an infinite space, since the energy is distributed more evenly between the two substrates.



A) Typical structure and size of VCSEL (cross section), B) Calculated thermal noise limit and measured frequency noise spectra in VCSEL. Experimental results a)⁸ and b)⁹ were scaled to $\lambda=1550\text{nm}$ to compare with the calculation. The experimental results were limited by the white noise above $\sim 1\text{kHz}$. For the calculation, we used the following parameters: effective cavity length= $5\mu\text{m}$, coating diameter= $8\mu\text{m}$, coating thickness= $5\mu\text{m}$, beam radius= $3\mu\text{m}$, substrate (gain chip) diameter= $30\mu\text{m}$, conductive layer thickness= $1\mu\text{m}$, substrate loss= 10^{-3} , coating loss= 10^{-3} , and conductive layer loss= 10^{-1} .

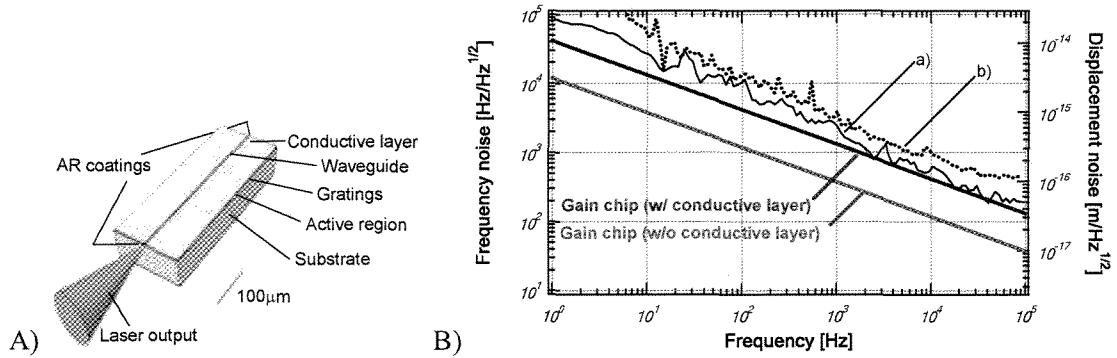


Figure 3| A) Typical structure and size of DFB laser (gain chip), B) Calculated thermal noise limit and measured frequency noise spectra in DFB laser. a)⁶ and b)¹⁰ show experimental results. For the calculation, we used the following parameters: effective cavity length=50μm, beam radius =1μm × 1.5μm, substrate (gain chip) size=200μm (W)×100μm (H)×400μm (L), conductive layer thickness=1μm, distance between conductive layer to the beam=2μm, substrate loss=10⁻³, and conductive layer loss=10⁻¹.

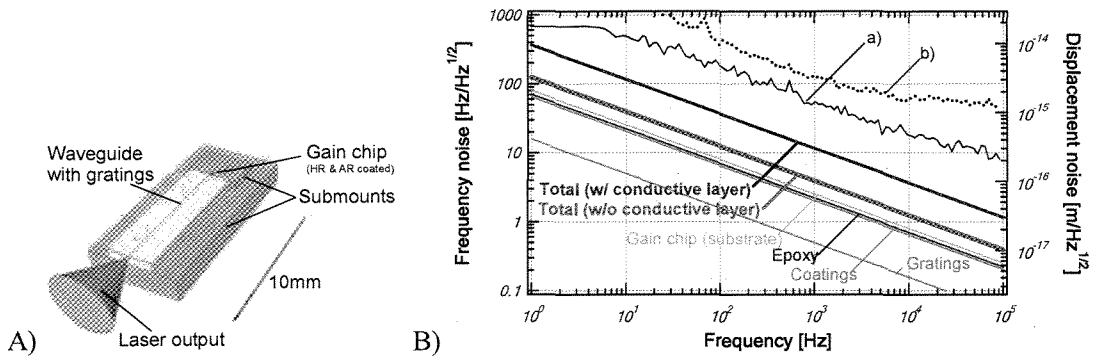


Figure 4| A) Typical structure and size of ECL, B) Calculated thermal noise limit and measured frequency noise spectra in DFB laser. a)¹⁰ and b)⁷ show experimental results. For the calculation, we used the following parameters: effective cavity length=5mm, beam radius in gain chip= $1.0\mu\text{m} \times 1.5\mu\text{m}$, beam radius in gratings= $5\mu\text{m}$, coating thickness= $8\mu\text{m}$, thickness of epoxy= $50\mu\text{m}$, thickness of conductive layer= $1\mu\text{m}$, distance between beam center and conductive layer center= $1.5\mu\text{m}$, substrate (gain chip) size= $200\mu\text{m}$ (W) $\times 100\mu\text{m}$ (H) $\times 400\mu\text{m}$ (L), mechanical loss of gain chip (substrate)= 10^{-3} , coating loss= 10^{-3} , grating loss= 10^{-4} , epoxy loss= 10^{-2} , conductive layer loss= 10^{-1} , and submount loss=0.